

FINAL PROJECT REPORT # 00064824

GRANT: DTRT13-G-UTC45
Project Period: 10/1/2018 – 12/31/19

Compacted Concrete Pavement

Participating Consortium Member:
Missouri University of Science and Technology

Authors:
Kamal Khayat, PhD, P.Eng
Nima Farzadnia, PhD
Missouri University of Science and Technology



RE-CAST:
REsearch on Concrete Applications for
Sustainable Transportation
Tier 1 University Transportation Center



DISCLAIMER

The contents of this report reflect the views of the authors, who are responsible for the facts and the accuracy of the information presented herein. This document is disseminated under the sponsorship of the U.S. Department of Transportation's University Transportation Centers Program, in the interest of information exchange. The U.S. Government assumes no liability for the contents or use thereof.

TECHNICAL REPORT DOCUMENTATION PAGE

| | | |
|--|---|---|
| 1. Report No. RECAST UTC # 00064824 | 2. Government Accession No. | 3. Recipient's Catalog No. |
| 4. Title and Subtitle Compacted Concrete Pavement | | 5. Report Date January 2020 |
| | | 6. Performing Organization Code: |
| 7. Author(s) Kamal Khayat and Nima Farzadnia | | 8. Performing Organization Report No. Project # 00064824 |
| 9. Performing Organization Name and Address RE-CAST – Missouri University of Science and Technology 500 W. 16 th St., 223 ERL Rolla, MO 65409-0710 | | 10. Work Unit No. |
| | | 11. Contract or Grant No. USDOT: DTRT13-G-UTC45 |
| 12. Sponsoring Agency Name and Address Office of the Assistant Secretary for Research and Technology U.S. Department of Transportation 1200 New Jersey Avenue, SE Washington, DC 20590 | | 13. Type of Report and Period Covered: Final Report Period: 10/1/2018 – 12/31/19 |
| | | 14. Sponsoring Agency Code: |
| 15. Supplementary Notes The investigation was conducted in cooperation with the U. S. Department of Transportation. | | |
| 16. Abstract Due to the increasing budget constraints and decreasing time in pavement construction, there has been renewed interest in exploring the application of cost-effective and rapid pavement construction techniques. Roller-compacted concrete (RCC) is a stiff mixture of aggregate, cementitious materials, and water, that is compacted by vibratory rollers [ACI 325, 1995]. Compacted concrete pavement (CCP) is an advanced form of RCC. CCP is comprised of similar proportions as that of RCC; however, it utilizes an admixture that enables better finishing and durable surface texture. The major difference in construction is that CCP has a longer “fresh” or “green” period and requires little or no rolling that makes the riding surface more uniform and consistent. The use of CCP technology is supposed to secure smooth texture during paving. Past research undertaken at Missouri University of Science and Technology (Missouri S&T) in collaboration with the Missouri Department of Transportation (MoDOT) for the investigating of in-situ properties of RCC mixtures demonstrated prospective application in pavement construction with acceptable performance [Khayat and Libre, 2014]. However, limited experience exists with CCP. This project investigated the performance of CCP designed with special design features and durability of surface texture that can reduce construction cost and secure safe and durable surface texture. Their fresh and hardened performance were evaluated, and pavement quality after construction was monitored periodically. | | |
| 17. Key Words Compacted concrete pavement | 18. Distribution Statement No restrictions. This document is available to the public. | |
| 19. Security Classification (of this report) Unclassified | 20. Security Classification (of this page) Unclassified | 21. No of Pages 37 |



Missouri University of Science and Technology
Civil, Architectural and Environmental Engineering Department

Compacted Concrete Pavement

Activity Report

Kamal Khayat, PhD, P.Eng

Nima Farzadnia, PhD

Progress Report

January 2020

1. Introduction

Due to the increasing budget constraints and decreasing time in pavement construction, there has been renewed interest in exploring the application of cost-effective and rapid pavement construction techniques. Roller-compacted concrete (RCC) is a stiff mixture of aggregate, cementitious materials, and water, that is compacted by vibratory rollers [ACI 325, 1995]. Compacted concrete pavement (CCP) is an advanced form of RCC. CCP is comprised of similar proportions as that of RCC; however, it utilizes an admixture that enables better finishing and durable surface texture. The major difference in construction is that CCP has a longer “fresh” or “green” period and requires little or no rolling that makes the riding surface more uniform and consistent. The use of CCP technology is supposed to secure smooth texture during paving.

Past research undertaken at Missouri University of Science and Technology (Missouri S&T) in collaboration with the Missouri Department of Transportation (MoDOT) for the investigating of in-situ properties of RCC mixtures demonstrated prospective application in pavement construction with acceptable performance [Khayat and Libre, 2014]. However, limited experience exists with CCP. This project investigated the performance of CCP designed with special design features and durability of surface texture that can reduce construction cost and secure safe and durable surface texture. Their fresh and hardened performance were evaluated, and pavement quality after construction was monitored periodically.

2. Research objectives

In order to assess the construction issues and characterize the long-term performance of the proposed CCP, three CCP test cells made with and without fiber as part of a larger project that were constructed in Scott County, Missouri, and designed and tested. Table 1 shows the typical characteristics of the three tested cells of CCP with different panel sizes with and without structural synthetic macro fibers (cells 1, 2, and 3). The total pavement width is 24 feet.

Table 1 - Typical characteristics of the three tested cells of CCP

| Item | Cell 1 | Cell 2 | Cell 3 |
|--------------------|-----------------------|-----------------------|--------------------------|
| Mixture | Control CCP | Control CCP | Fiber-reinforced CCP |
| Fiber content (%) | 0 | 0 | Minimum 20% (ASTM C1609) |
| Length (ft) | 500 | 500 | 250 |
| Panel size (WxLxT) | 24 ft × 15 ft × 6 in. | 24 ft × 12 ft × 6 in. | 24 ft × 15 ft × 6 in. |
| Joint size (in.) | 0.125 in. × T/4 | 0.125 in. × T/4 | 0.125 in. × T/4 |

The study aimed at determining the performance of designed CCP mixtures given special design features and durability of surface texture through field implementation and detailed laboratory testing. The primary performance characteristics included mechanical properties, drying shrinkage, durability, and enhancement of joint load transfer gained from fiber-reinforcement of the pavement. The various field and laboratory research tasks that were undertaken by Missouri S&T are elaborated below. Table 2 summarizes the testing program that were conducted in this proposed research.

Table 2 - Experimental testing

| Evaluated performance | Cell 1 or 2 | Cell 3 | Sample size | Test method | |
|---|-------------|----------|-------------|---------------------------|------------|
| Construction/instrumentation | | | | | |
| Install sensors | x | x | | | |
| Sampling preparation | | | | | |
| Cut samples from additional 15-foot sections (noted in M2-C) | x | x | | | |
| Create research test samples from fresh concrete during pavement construction | x | x | | ASTM C1435 | |
| Lab testing of saw-cut and cored samples | | | | | |
| | | No. | No. | Size | |
| Compressive strength (7, 28, 56 d) (N = 3) | x | 9 | x 9 | 3 × 6" Cores | ASTM C39 |
| Flexural strength of CCP without fiber (7, 28, 56 d) (N = 3) | x | 9 | | 6 × 6 × 22" prisms | ASTM C78 |
| Flexural strength of FRC (7, 28, 56 d) (N = 3) | | | x 9 | 6 × 6 × 22" prisms | ASTM C1609 |
| Freeze-thaw durability (N = 3) | x | 3 | x 3 | 3 × 4 × 16" prisms | |
| Hardened air content and spacing factor (N = 2) | x | 3 | x 3 | Part of 4" cores (4 × 1") | ASTM C457 |
| 56-d permeability RCPT (N = 3) | x | 3 | x 3 | Part of 4" cores (4 × 2") | ASTM C1202 |
| Deicer salt scaling (N = 2) | x | 2 | x 2 | 11 × 10 × 3" slabs | ASTM C 672 |
| Bulk resistivity (N = 2) | x | 2 | x 2 | 4" cores | ASTM C1760 |
| Drying shrinkage (after 7 d moist curing, 180 d dry curing) (N = 3) | x | 3 | x 3 | 3×3× 11.3" prisms | ASTM C 157 |
| Total no. of samples | | 34 | 34 | | |
| Lab testing of samples prepared during pavement construction | | | | | |
| | | No. | No. | Size | |
| Compressive strength (7, 28, 56 d) (N = 3) | x | 6-9 | x 6-9 | 6 × 12" Cylinders | ASTM C39 |
| Flexural strength of CCP without fiber (7, 28, 56 d) (N = 3) | x | 6-9 | | 6 × 6 × 22" prisms | ASTM C78 |
| Flexural strength of FRC (7, 28, 56 d) (N = 3) | | | x 6-9 | 6 × 6 × 22" prisms | ASTM C1609 |
| Coefficient of thermal expansion (N = 3) | x | 3 | x 3 | 4 × 8" cylinders | |
| Total no. of the samples | | Up to 21 | Up to 21 | | |

3. Project operation

3.1. Test strip

The paving of the test strip was initiated at 1 pm on October 24th, 2018 in Scott County, Missouri. Figure 1 shows the location of the project. Figures 2 and 3 shows the paving process implemented

using a concrete slip-form paving equipment. As indicated in Figure 3 the surface alignment was tested constantly, and the paver was adjusted accordingly.

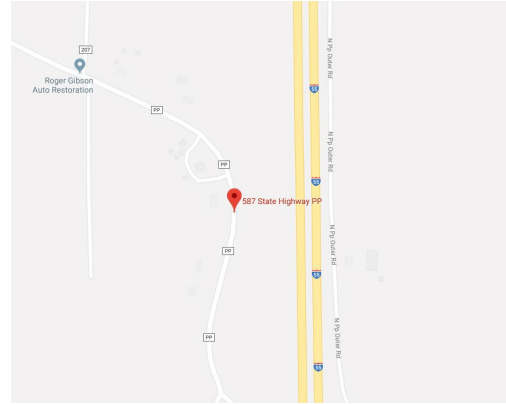


Figure 1 - Project location: 587 State Hwy PP Scott City, MO 63780



Figure 2 - Paving process



Figure 3 - Surface adjustments

The density test was conducted with a non-destructive method Nuclear Density Meter Ground Test Equipment at both sides of the pavement. Nuclear density gauge measures in-place density using gamma radiation. Gamma rays are emitted from the source and interact with electrons in the pavement through absorption, Compton scattering, and the photoelectric effect. A Geiger-Mueller detector (situated in the gauge opposite from the handle) counts gamma rays that reach it from the source. Pavement density is then correlated to the number of gamma rays received by the detector (<http://www.troxlerlabs.com>).



Figure 4 - Density measurement

The test results showed that the density was not uniformly distributed. For the test strip, the amendments were made using addition of concrete and further compaction, as shown in Figure 5.



Figure 5 - Density adjustments

Even after the further compaction, visual observation of the cross section of the pavement (Figure 6) showed that the pavement was less dense at both ends, while the compaction was effective at the center. The cast CCP was poor in paste at some parts. Therefore adjustment in the mix design were made accordingly.



Figure 6 - Visual observation of the cross section

3. 2. Instrumentation

The sensor installation and instrumentation, including sensors of strain due to environment, dynamic load response, and joint opening, with minimal disturbance to grade were carried out by MnDOT. Figure 7 shows the instrumentation of cells 1, 2 and 3.



Figure 7 - Instrumentation operation

The applied sensors and gauges are shown in Figure 8. A brief description of each sensor is given in Table 3. Figure 9 Illustrates the instrumentation schematics that were used.



Thermocouple Tree,

Joint Opening Block Out

Vibr. Wire Strain Gauges

Dynamic Strain Gauges

Figure 8 - Sensors and gauges applied in Cell 1, 2 and 3

Table 3 - The instrumented sensors in Cells 1, 2 and 3

| Item | Sensor | Description |
|------|------------------------------|---|
| 1 | Thermocouple Tree | To measure frost depth, temperature gradients in pavement layers and temperature compensation for other instruments |
| 2 | Joint Opening Block Out | Placed within 1-inch PVC conduit, which is held within a joint opening block out that crosses the joint between the two panels for measurement of the displacement of the pavement joint. |
| 3 | Vibrating Wire Strain Gauges | Two gauges has been placed in the longitudinal and transverse direction of the pavement to evaluate the effects of both directions for determining effects of applied loads to the pavement |
| 4 | Dynamic Strain Gauges | Two more dynamic strain gauges are placed near the edge of the pavement in the longitudinal direction to measure the edge deflection due to traffic loads. |

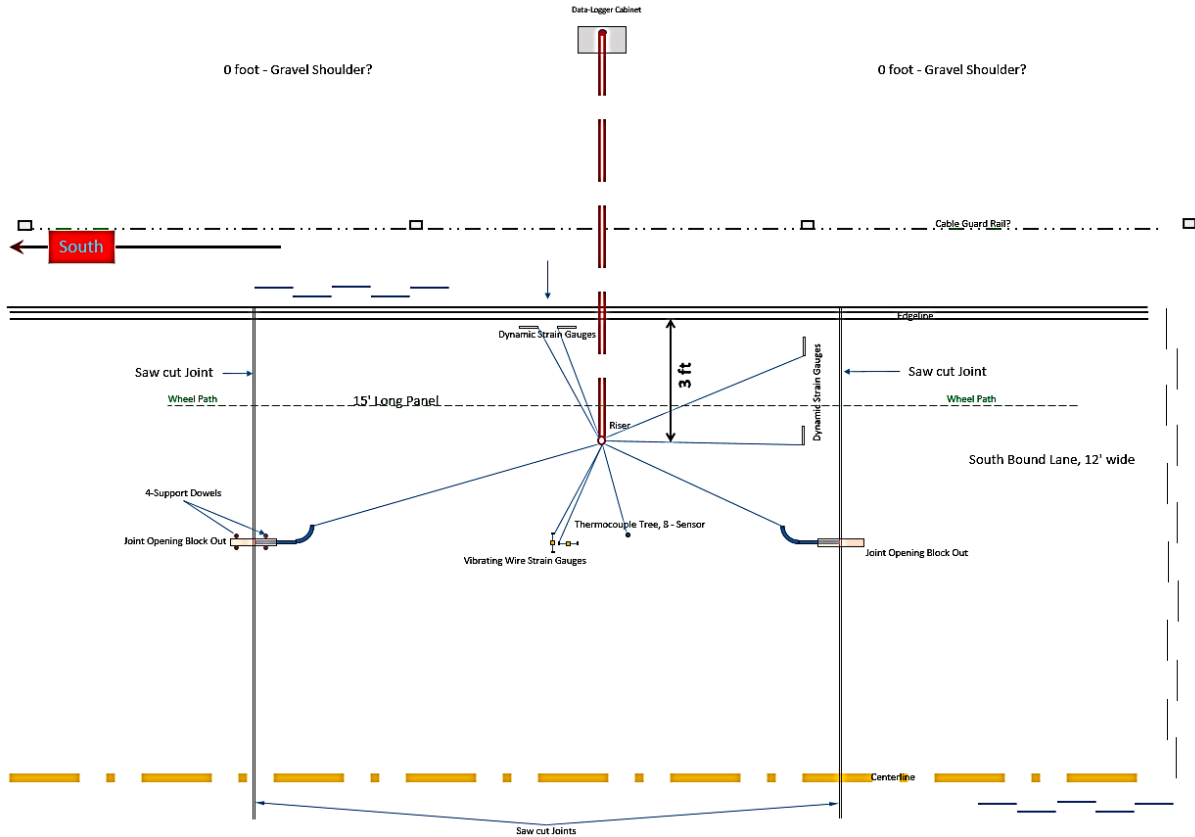


Figure 9 - Instrumentation schematics (plan)

3.3. Paving operation

Paving operation started at 12 pm on 25th of October 2018. The project was initially on hold due to precipitation. Figures 10 to 12 illustrate phases associated to loading of the paver, compaction and measurements, and surface finishing. Curing in a form of spray was then applied, as shown in Figure 12.



Figure 10 - Loading process of the slip-form paving

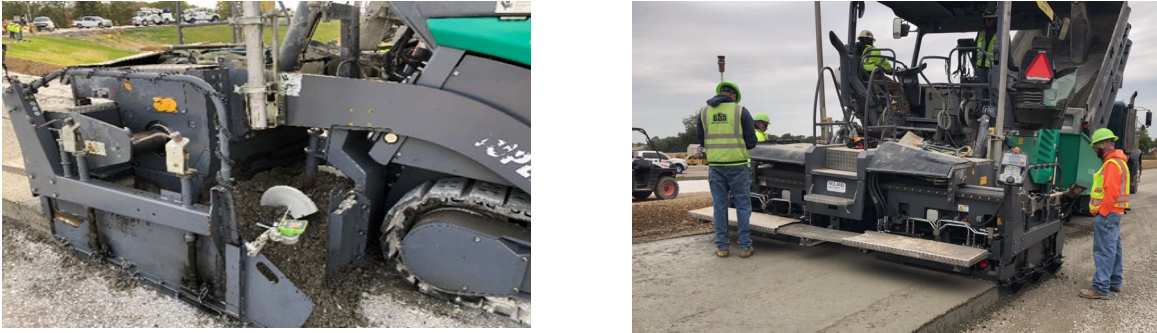


Figure 11 - Paving and adjustments



Figure 12 - Finishing process

3.5. Sampling

Cast in filed Mixtures were prepared on the plant site at I-55, Scott City, MO on October 25, 2018 (Figure 13)

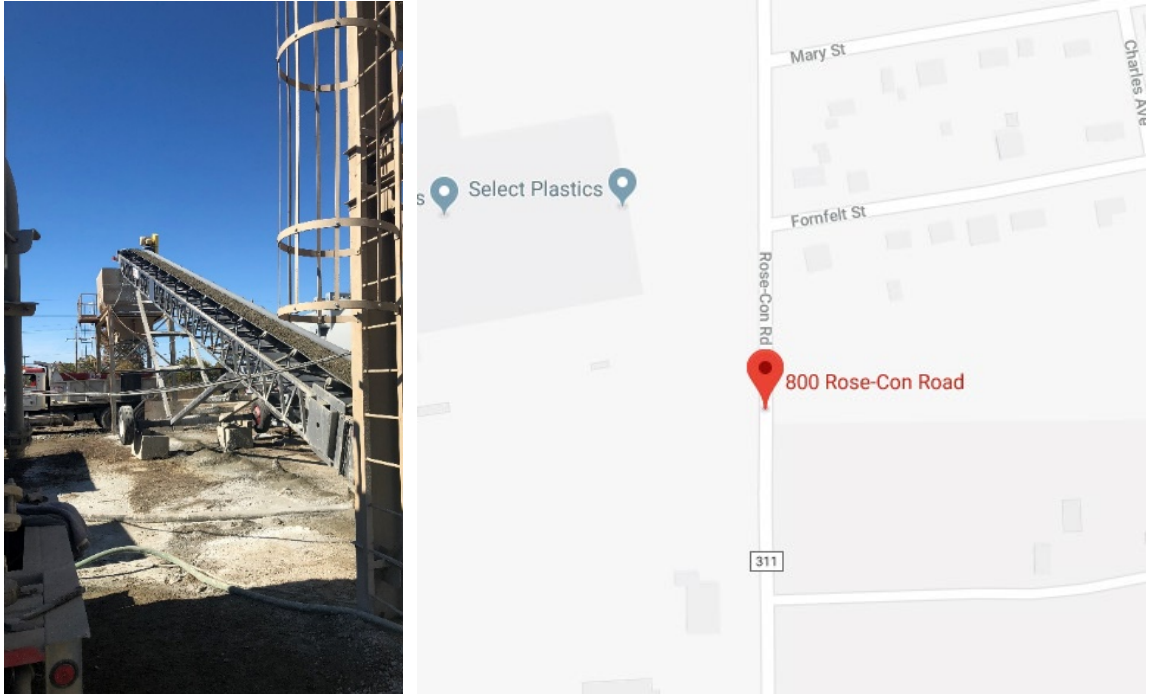


Figure 13 - Location of the plant site: 800 Rose-Con Rd Scott City, MO 63780

Two mixtures were sampled in 18 prism molds (6" ×6" ×24") for flexural test and 18 cylindrical molds (6" ×12") to test in compression. Mixture 1 represented Cells 1 and 2 as the base mixture without any fiber, while mixture 3 was reinforced with 5 pcy of fibers as in Cell 3. The moisture content was maintained between 5-6% with water-to-cementitious materials ratio (w/cm) between 0.31-0.38. Figure 14 shows the sampling operation.



Figure 14 - Sampling

During sampling, Vebe consistency time and density of compacted concrete with and without fiber were measured, as per Procedure A, ASTM C 1170. The Vebe test setup is shown in Figure 15. The procedure is described in details in Section 4.1



Figure 15 – Vebe test apparatus for determining consistency/density of fresh CCP

Compaction was adequately provided by a jackhammer using rectangular plates of 5.75” ×8” and circular plates of 5.75” in 3 and 4 layers for prism and cylindrical molds, respectively (Figure 16). The compaction of cylindrical samples was in compliance with ASTM C 1435.



Figure 16 - Compaction tools and process

The samples were covered with wet burlaps, followed by plastic bags and blankets to maintain appropriate curing moisture and temperature. Figure 17 shows the maintenance of the samples after casting and prior to transport to laboratory in Missouri S&T.



Figure 17 - Maintenance of samples before transport to Missouri S&T

On October 29th, the samples were demolded and transported to Missouri S&T. The transportation was done in compliance with ASTM C 31. Accordingly, samples were protected with sand as suitable cushioning material in boxes to prevent damage from jarring. And to prevent moisture loss during transportation, samples were wrapped with wet burlap. Transportation time was within 4 h as allowed by the ASTM code. Figure 18 shows the demolding and transporting of the samples.



Figure 18 - demolding and transportation of samples

The samples were cured in standard curing conditions prior to the testing day. The cylindrical samples were capped according to ASTM C 617 using Sulphur mortar (Figure 19).



Figure 19 - Capping process of cylindrical samples

4. Testing procedure and results

This section reports results from various field and laboratory tests on primary performance characteristics of CCP that were undertaken by Missouri S&T. The primary performance characteristics included fresh properties, mechanical properties (compressive and flexural strengths), drying shrinkage, and durability (freeze-thaw durability, 56-d rapid chloride permeability, deicer salt scaling, and hardened air-void system). Throughout the report Mixture 1 and Mixture 2 denote the CCP without fiber (Cells 1 and 2) and CCP with fiber (Cell 3), respectively.

4.1 Vebe test (consistency time and density)

The Vebe consistency time and density of fresh compacted concrete were measured during the paving in compliance with ASTM C 1170. The procedure consists of placing a representative sample of CCP mixture of approximately 29.5 lb (13.5 kg) in a standardized cylindrical steel mold. The mold was fixed on a vibrating table, and a circular plastic plate was placed on top of the concrete sample. In order to consolidate the concrete, a removable mass of 50 lb (22.7 kg) was applied to the plate, and the vibrating table was turned on. Figure 20 shows the Vebe test apparatus for determining consistency/density of fresh CCP.

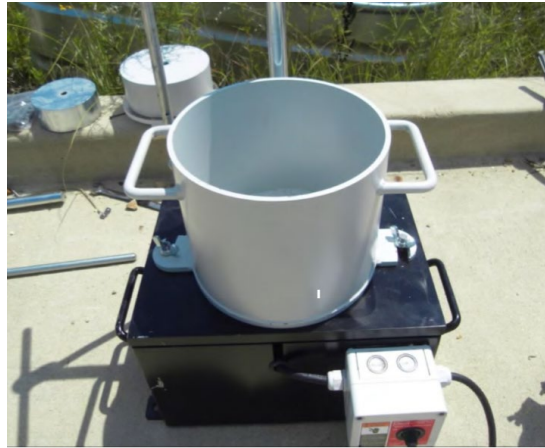


Figure 20 - Vebe test

For Vebe consistency time, the time of consolidation was recorded as the consistency time until a mortar ring was observed around the plastic plate. In the absence of mortar ring formation within 60 seconds from the start of vibration, the Vebe consistency time was reported to be greater than 60 seconds. The density of fresh compacted concrete was calculated after the Vebe consistency time test. The mold was overfilled with more concrete, properly consolidated until the concrete was just above the mold. The density of fresh compacted concrete was measured using the mass of mold with concrete and the mass and volume of the empty mold. Table 4 shows the Vebe test results for mixtures associated to Cells 1 and 2, and 3, respectively.

Table 4 - Vebe test results

| Mixture properties | Mixture 1 (No fiber) | Mixture 2 (with fiber) |
|---|-------------------------------|-------------------------------|
| Vebe consistency time (sec) | > 60 | > 60 |
| Density of fresh compacted concrete (lb/ft ³) | 124 (1978 kg/m ³) | 142 (2272 kg/m ³) |

Based on the observation during the Vebe test of both mixtures, the mortar ring was not formed around the total perimeter of the surcharge within 60 s from the start of vibration. Therefore, the Vebe consistency time for both representative samples were reported to be greater than 60 s. Accordingly, both tested mixtures (with and without fibers) are categorized to have extremely dry consistency, as per ASTM C1170. However, the test results showed that the incorporation of fibers increased the density of the fresh CCP by 15%.

4. 2. Compressive strength

The compressive strength test was conducted in compliance with ASTM C39. All cylinders were capped one day before the testing using high-strength Sulphur capping compound according to ASTM C 617. They were returned into a moist curing room until the testing age. The samples were maintained in saturated conditions until the time of testing. Compressive strength test was done in compliance with ASTM C39 on 6×12” samples (total of 6 cylinders). The stress rate was 0.25 ± 0.05 MPa/s [35 ± 7 psi/s]. Table 5 shows the compressive strength results of cast-in-filed Mixtures 1 and 2 at 7, 28, 91 days and saw-cut Mixtures 1 and 2 at 91, 120, 180 days.

The compressive strength of both Mixtures 1 and 2 increased with increase of curing time. For example, the increase of curing time from 7 d to 91d resulted in 104% and 20% higher compressive strength for cast-in-place Mixtures 1 and 2, respectively. The increase in curing time from 91 to 180 d resulted in 88% and 75% higher compressive strength of saw-cut Mixture 1 and 2, respectively. The compressive strengths of cast-in-field samples were greater than saw-cut samples, which can be related to the different compaction energy applied during sampling of cast-in-field samples. For example, the compressive strength of 91d cast-in-field Mixtures 1 and 2 was 41% and 39% greater than that of saw-cut specimens at the same age. However, results showed that the compressive strength of mixture with 5% pcy fiber was greater than that of without fiber for both cast-in-field and saw-cut samples.

Table 5 Compressive strength of samples

| | Mixture ID | Curing age (d) | Compressive strength 6”×12” cylinders (psi) | | | | Coefficient of variation |
|----------------------|-------------------------|----------------|---|------|------|-------------|--------------------------|
| | | | 1 | 2 | 3 | Average | |
| Cast-in-field sample | Mixture 1 (No fiber) | 7 | 1650 | 1560 | * | 1605 | 3% |
| | Mixture 2 (5 pcy fiber) | 7 | 4068 | 4370 | * | 4220 | 5% |
| | Mixture 1 (No fiber) | 28 | 3726 | 3609 | * | 3667 | 2% |
| | Mixture 2 (5 pcy fiber) | 28 | 5037 | 4874 | * | 4956 | 3% |
| | Mixture 1 (No fiber) | 91 | 3268 | 3373 | 3186 | 3276 | 1% |
| | Mixture 2 (5 pcy fiber) | 91 | 4424 | 5562 | 5198 | 5061 | 3% |
| Saw cut sample | Mixture 1 (No fiber) | 91 | 1918 | 1806 | 2070 | 1931 | 4% |
| | Mixture 2 (5 pcy fiber) | 91 | 3462 | 3461 | 2750 | 3103 | 5% |
| | Mixture 1 (No fiber) | 120 | 2545 | 3185 | * | 2865 | 6% |
| | Mixture 2 (5 pcy fiber) | 120 | 3720 | 3620 | * | 3670 | 2% |
| | Mixture 1 (No fiber) | 180 | 3770 | 3510 | * | 3640 | 3% |
| | Mixture 2 (5 pcy fiber) | 180 | 5625 | 4980 | 5700 | 5435 | 7% |

Note: * denotes poorly consolidated samples.

4.3. Flexural behavior results

The flexural strength test was conducted on prismatic samples measuring 6”x6”x24” (span of 18”) according to ASTM C1609. The loading rate was maintained at displacement control of 0.0035 in. /min until reaching a deflection of 0.02”. The rate of loading was then increased to 0.012 in. /min until failure. Figure 21 shows the test set-up for the flexural test.

The flexural strength was calculated as follows:

$$F = PL/bd^2 \quad (\text{Eq. 1})$$

where F is the strength (psi); P is the load (lbf); L is the span (in.); b is the average width of the sample (in.); d is the average depth of the sample (in.).

The residual strength was calculated by using the residual load in Eq. 1. The residual loads were determined at deflections of L/600 and L/150, respectively, according to Figure 22.



Figure 21 - Third-point flexural testing setup

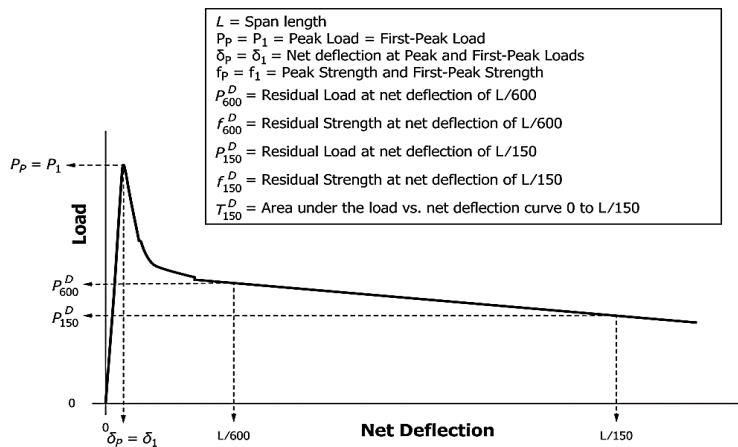


Figure 22 - Example of parameter calculations for first-peak load equal to peak load (ASTM C1609)

The load-deflection results of the two tested cast-in-filed Mixtures 1 and 2 at 7, 28, 91 days and saw-cut Mixtures 1 and 2 at 91, 120, 180 days are reported in Figure 23 and 24, respectively. The samples of Mixture 1 showed brittle failure behavior. Mixture 1 failed abruptly after reaching the peak load. The fibrous mixture had sharp drops in load carrying capacity but maintained residual

strength until a deflection of 0.12 in. Furthermore, the peak load of 91-d cast-in-place samples was greater than that of saw-cut specimens.

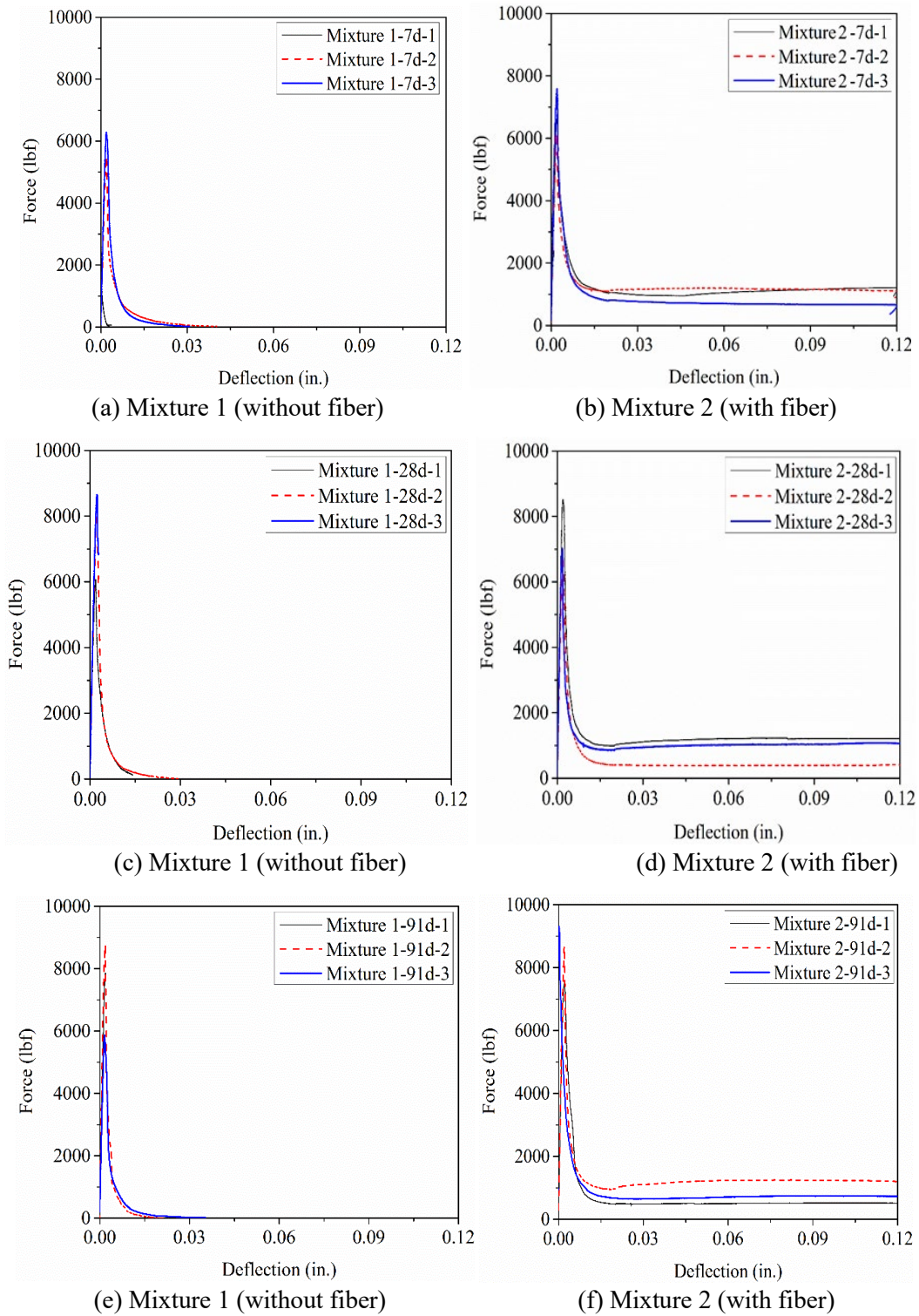


Figure 23 - Load-deflection curves of three field-cast prismatic samples of the two investigated mixtures at 7, 28, and 91 days

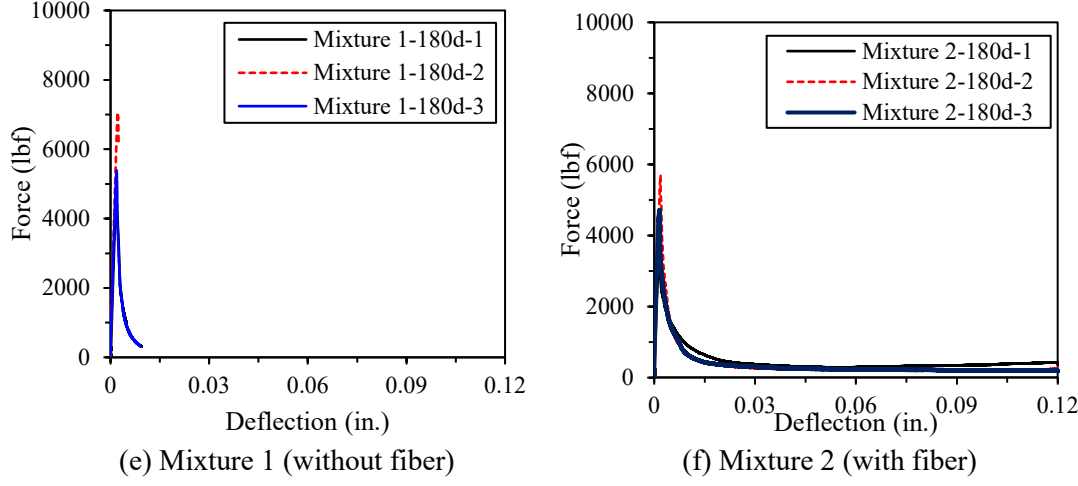
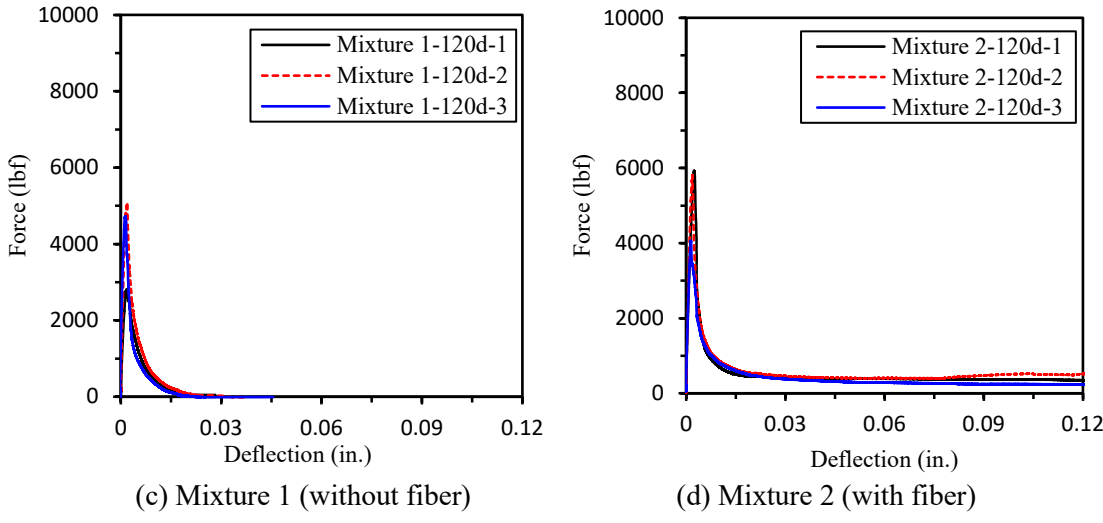
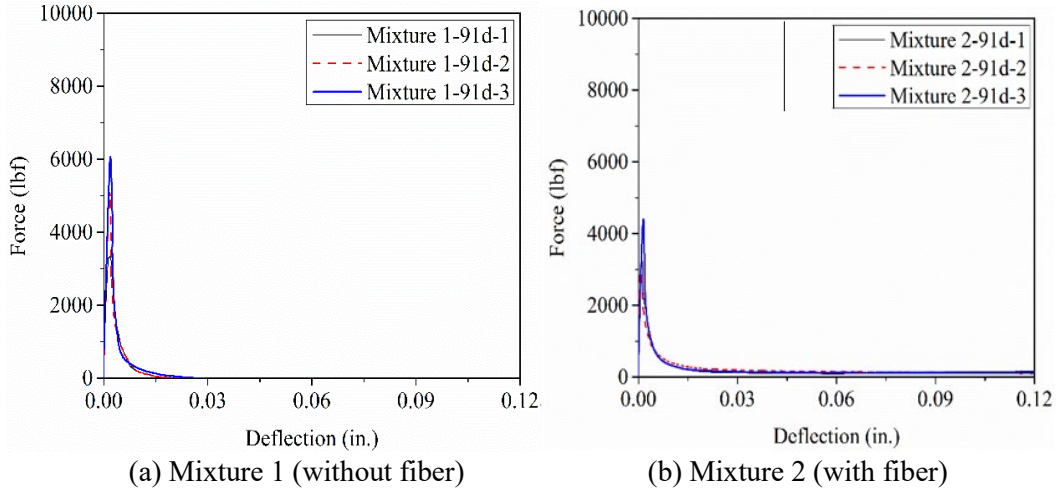


Figure 24 - Load-deflection curves of three saw-cut prisms of the two investigated mixtures at 91, 120, and 180 days

Table 6 shows the flexural strength and residual strength values of the Mixture 1 at curing age of 7, 28, 91 d and Mixture 2 at curing age of 91, 120, 180 d. The flexural strength of Mixtures 1 and

2 improved with curing time. For example, the increase in curing time from 7 to 91 d resulted in 22% and 17% increase in flexural strength of cast-in-field samples. The increase in curing time from 91 to 180 d resulted in 31% and 41% increase in flexural strength of saw-cut specimens. The incorporation of fibers slightly increased flexural strength of Cast-in field samples, while the flexural strength slightly decreased for saw-cut specimens. For example, the incorporation of fiber increased the flexural strength from 555 to 685 MPa for cast-in-place samples, while using fiber in saw-cut specimens decreased flexural strength from 404 to 295 MPa. This can be attributed that the incorporation of fiber caused difficulty on compaction. However, well-compacted fiber reinforced concrete can increase the flexural strength.

Table 6 - Flexural and residual strength results

| | Mix. ID | Flexural strength | | | | | Residual strength at a deflection of L/600 (0.03") | | | | Relative residual strength ratio | Residual strength at a deflection of L/150 (0.12") | | | | Relative residual strength ratio |
|---|-------------|-------------------|-----|-----|------------|-----|--|----|----|-----------|----------------------------------|--|----|----|-----------|----------------------------------|
| | | (psi) | | | | | (psi) | | | | (%) | (psi) | | | | (%) |
| | | Sample | 1 | 2 | 3 | Ave | COV (%) | 1 | 2 | 3 | Ave | Ave | 1 | 2 | 3 | Ave |
| C | Mix. 1-7d | 402 | 483 | 419 | 435 | 10 | 0 | 0 | 0 | 0 | 0 | 0 | 0 | 0 | 0 | 0 |
| | Mix. 2-7d | 481 | 438 | 539 | 486 | 10 | 92 | 75 | 47 | 71 | 15 | 75 | 83 | 55 | 71 | 15 |
| | Mix. 1-28d | 466 | 616 | 664 | 582 | 18 | 0 | 0 | 0 | 0 | 0 | 0 | 0 | 0 | 0 | 0 |
| | Mix. 2-28d | 555 | 655 | 563 | 591 | 9 | 85 | 33 | 75 | 64 | 11 | 88 | 32 | 89 | 70 | 12 |
| | Mix 1 - 91d | 665 | 728 | 400 | 555 | 7 | 0 | 0 | 0 | 0 | 0 | 0 | 0 | 0 | 0 | 0 |
| | Mix 2 - 91d | 582 | 724 | 745 | 685 | 12 | 37 | 92 | 52 | 60 | 9 | 40 | 99 | 58 | 66 | 10 |
| S | Mix 1 - 91d | 280 | 430 | 505 | 404 | 23 | 0 | 0 | 0 | 0 | 0 | 0 | 0 | 0 | 0 | 0 |
| | Mix 2 - 91d | 270 | 245 | 365 | 295 | 18 | 10 | 15 | 12 | 13 | 5 | 13 | 8 | 10 | 10 | 3 |
| | Mix 1-120 | 265 | 825 | 445 | 515 | 45 | 0 | 0 | 0 | 0 | 0 | 0 | 0 | 0 | 0 | 0 |
| | Mix 2-120 | 540 | 525 | 370 | 480 | 16 | 32 | 43 | 30 | 35 | 7 | 26 | 38 | 19 | 28 | 6 |
| | Mix 1-180 | 425 | 825 | 510 | 585 | 29 | 0 | 0 | 0 | 0 | 0 | 0 | 0 | 0 | 0 | 0 |
| | Mix 2-180 | 310 | 515 | 430 | 415 | 20 | 28 | 21 | 24 | 24 | 12 | 29 | 19 | 14 | 21 | 5 |

Note. C: cast-in-field; S: saw-cut; Ave: average; and COV: coefficient of variation.

4.4. Rapid chloride permeability test (RCPT)

The chloride permeability of samples measuring 4"×2" was evaluated for saw-cut samples in accordance with ASTM C1202. Figure 25 shows the testing apparatus. The permeability scale for chlorides and the tested results are summarized in Tables 7 and 8. The results represent the average value of three samples for each mixture. The values of charge passed for the Mixtures 1 and 2 were 3740 and 5090 Coulomb, respectively. This indicates that the Mixture 2 had a high electrical conductivity, while the Mixture 1 exhibited a moderate electrical conductivity. The higher RCPT

value for the Mixture 2 might be due to the higher level of pores caused by a porous interfacial zone around the fibers.



Figure 25 - Testing apparatus for RCPT

Table 7 - Permeability scale for chlorides as per ASTM C1202

| Passed charge | Permeability |
|---------------|--------------|
| > 4000 | High |
| 2000-4000 | Moderate |
| 1000-2000 | Low |
| 100-2000 | Very low |
| <100 | Negligible |

Table 8 - RCPT results for saturated cores

| Permeability | Q (Coulomb) |
|--|-------------|
| Mixture 1 (without fibers) | 3740 |
| Mixture 2 (with fibers) | 5090 |
| $Q = 900 (I_0 + 2I_{30} + 2I_{60} + \dots + 2I_{330} + I_{360})$ Q: Charge passed. I ₀ : current immediately after the applied voltage. I _t : current at t min after the applied voltage. | |

4.5. Bulk/Surface electrical resistivity

Surface electrical resistivity of samples was measured in accordance with AASHTO T95. The surface resistivity test method consisted of measuring the resistivity of 4" × 6" cores using a four-point Wenner probe array, as illustrated in Figure 26. An AC potential difference was applied in the outer pins of the Wenner array generating current flow in the concrete. The potential difference generated by this current was measured using the two inner probes. The current used and potential obtained along with the area affected were used to calculate the resistivity of cores. Bulk resistivity was also conducted on the same cored samples in compliance with ASTM C1760. In this method, bulk electrical resistivity was measured as the voltage between the two ends of cores as a small AC current was applied. The surface and bulk resistivity of concrete samples at the age of 91 days were measured for two samples of each mixture, and the average value is reported.

The surface and bulk resistivity values of the two investigated mixtures are shown in Tables 8 and 9 as KΩ.cm, respectively. Mixtures 1 and 2 showed almost similar bulk resistivity values, which

were 9.6 and 9.2, respectively. The surface resistivity was 52.8 and 44.1 K Ω .cm, respectively. The results are conclusive that the inclusion of fiber to the mixture increased the electrical resistivity.



Figure 26 - Testing apparatus for surface resistivity (left) and bulk resistivity (right)

Table 9 - Bulk electrical resistivity of the two investigated mixtures (K Ω .cm)

| Mix ID | 1 | 2 | 3 | 4 | 5 | 6 | 7 | Ave. | Ave. |
|---------|------|------|------|------|------|------|------|------|------------|
| Mix 1-1 | 8.2 | 8.3 | 7.6 | 11.1 | 13 | 12.3 | 10.7 | 10.2 | 9.6 |
| Mix 1-2 | 10 | 10.7 | 10.6 | 10.1 | 7.9 | 7.2 | 7.5 | 9.1 | |
| Mix 2-1 | 8.6 | 7.2 | 7.5 | 7.2 | 6.8 | 7.2 | 7.8 | 7.5 | 9.2 |
| Mix 2-2 | 10.9 | 10.7 | 11 | 10.8 | 11.2 | 10 | 11.4 | 10.9 | |

Table 10 - Surface electrical resistivity of two investigated mixtures (K Ω .cm)

| Mixture ID | Measure 1 | Measure 2 | Measure 3 | Ave. | Ave. |
|-------------|-----------|-----------|-----------|------|-------------|
| Mixture 1-1 | 53.8 | 49.7 | 55.2 | 52.9 | 52.8 |
| Mixture 1-2 | 52.6 | 53.4 | 51.8 | 52.6 | |
| Mixture 2-1 | 47.8 | 46.5 | 46.9 | 47.1 | 44.1 |
| Mixture 2-2 | 42.9 | 38.5 | 41.7 | 41.0 | |

4.6. Air-void system

Samples measuring 4" \times 1" cut from cores were prepared to determine the air-void system according to ASTM C 457. Two samples for each mixture were tested. The time required for the measurement of each sample was about 10 min on average. Figure 27 shows sample preparation for air-void system analysis. Each sample was tested four times, rotating the sample by 90° each time, and the average of the four results was calculated as the air-void system parameters for that sample. By this means, the variations in the results would be averaged out, and more reliable values would be obtained.





Figure 27 – Sample preparation for air-void system analysis

Table 11 presents the air-void system parameters of the two investigated mixtures. The air voids of the Mixtures 1 and 2 were 4.03% and 5.12%, respectively. The greater air-void content of the Mixture 2 agrees well with results of RCPT (Table 8).

Table 11 - Air void content and spacing factor of the two investigated mixtures

| Property | Mixture 1 (without fibers) | Mixture 2 (with fibers) |
|----------------------------|----------------------------|-------------------------|
| Air Content (%) | 4.03 | 5.12 |
| Average Chord Length (in.) | 0.005 (0.13 mm) | 0.006 (0.15mm) |
| Paste to Air Ratio | 6.25 | 5.52 |
| Spacing Factor (in.) | 0.006 (165 μ m) | 0.007 (175 μ m) |

4.7. Freeze-thaw resistance

The freeze-thaw resistance of saw-cut samples was evaluated in accordance with ASTM C666, Procedure A. The test procedure consisted of subjecting concrete samples to 300 cycles of rapid freezing and thawing in water at temperatures varying between 41 to -0.4 °F. For each mixture, three samples were tested and the average was used to interpret the results. The samples were placed in metal containers and surrounded by approximately 0.2 in. of clean water in a specified chamber. Freezing was generated with a cooling plate at the bottom of the apparatus, whereas thawing was produced by heating elements placed between the containers. The dynamic modulus of elasticity of samples subjected to freeze-thaw cycles was measured.

Figure 28 shows the variations of dynamic modulus of elasticity during 220 cycles of saw-cut samples taken from the fiber-reinforced and non fiber-reinforced concrete pavements. For each concrete type, three samples were extracted from various locations in the pavement. Test results showed that the relative dynamic modulus gradually decreased for Mixtures 1 and 2 with the increase of freeze-thaw cycles. For each concrete type, the changes in dynamic modulus of elasticity were significantly different. This can reflect the uneven degree of consolidation of the concrete.

The durability coefficient was calculated as the square of the ratio of pulse velocities of P waves in the concrete at the end of the testing period to the value recorded at the beginning of the test, multiplied by the number of cycles at the termination of the test divided by 300. The test was terminated soon after the relative dynamic modulus of elasticity decreased to a level lower than 60%. Test results showed that the incorporation of fibers did not have a significant effect on frost

durability. The relative dynamic modulus of elasticity at 220 cycles was 56% for Mixture 2, which translates into a durability coefficient of 41%. These values were 53% and 39% for Mixture 1, respectively. This indicates poor frost durability for both mixtures used in the CCP project.

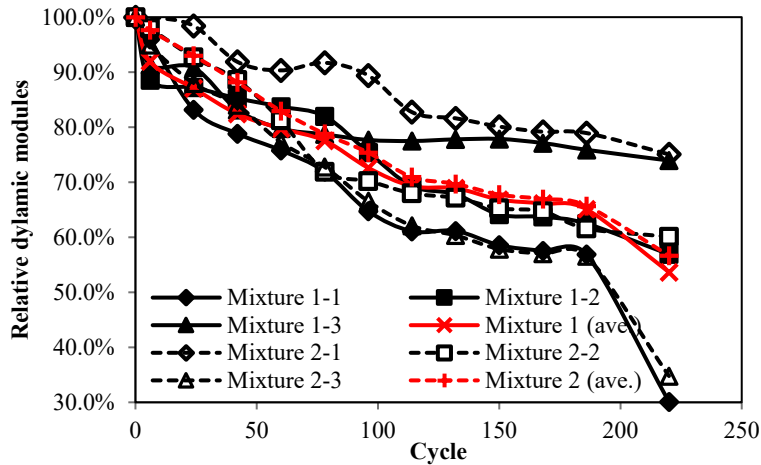


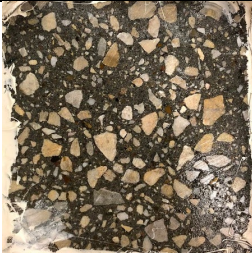






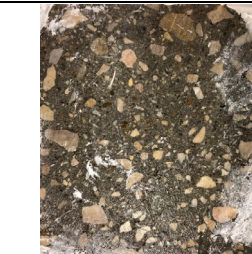


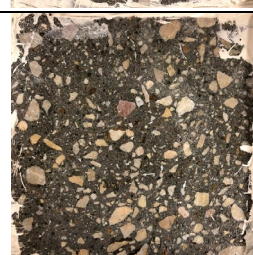
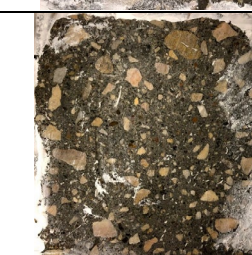


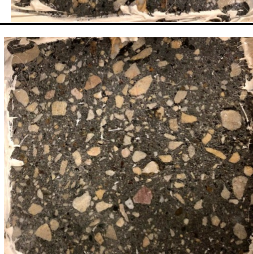
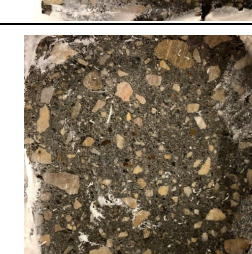

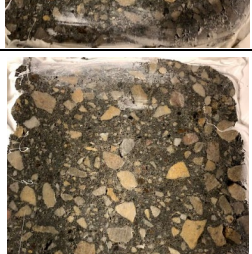





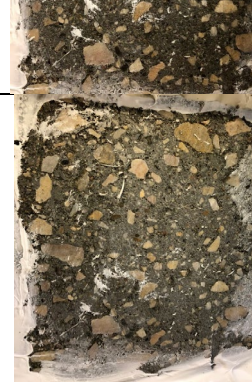
Figure 28 - Variations of relative dynamic modulus of elasticity of Mixture 1 (without fibers) and Mixture 2 (with fibers) determined on saw-cut samples



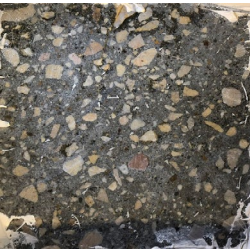




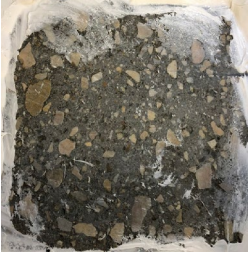



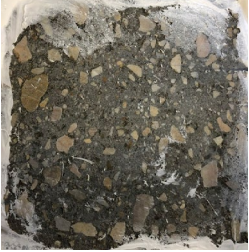
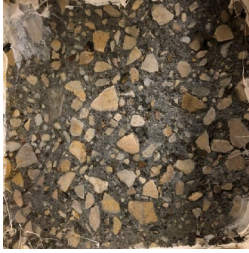


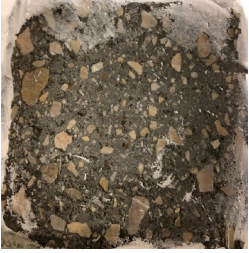





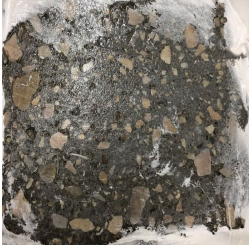


4.8. Deicing salt-scaling resistance

Deicing salt scaling test was carried out using three saw-cut slabs measuring 11"×10"× 3" for Mixtures 1 and 2 in accordance with ASTM C672. The test was conducted on two samples representing each mixture at the 91 days. During this test, the surface of the concrete was covered with approximately 6 mm of 4% sodium chloride solution (i.e., 0.14 oz. of NaCl for each (3.4 fl. oz.) of water). The samples were subjected to 80 freezing and thawing cycles by alternately placing them in a freezing environment (-0.08 ± 3.02 °F) and a thawing environment (73.4 ± 3.1 °F). At the end of each series of 5 cycles, the salt solution was renewed, and the scaling residues were recuperated, dried, and weighed. The extent of surface scaling was assessed visually. The visual rating of zero means no scaling for concrete surfaces and five for severe scaling with coarse aggregates visible over the entire surface. The visual ratings of the concrete surface before testing and after 80 cycles of freeze-thaw shown in Table 12. No visible scaling was observed during 80 cycles indicating acceptable resistance of the mixture to salt scaling.

Table 12 - Saw-cut slabs before and after exposure to salt scaling (80 cycles)

| | Mixture 1-1 | Mixture 1-2 | Mixture 2-1 | Mixture 2-2 |
|---------|-------------|-------------|-------------|-------------|
| Initial | | | | |

| | | | | |
|--------------|---|---|--|---|
| 5 cycles |  |  |  |  |
| 10 cycles |  |  |  |  |
| 15 cycles |  |  |  |  |
| 20 cycles |  |  |  |  |
| 25 cycles |  |  |  |  |
| 35 cycles |  |  |  |  |

| | | | | |
|--------------|---|---|--|---|
| 40 cycles |  |  |  |  |
| 45 cycles |  |  |  |  |
| 50 cycles |  |  |  |  |
| 55 cycles |  |  |  |  |
| 60 cycles |  |  |  |  |
| 65 cycles |  |  |  |  |

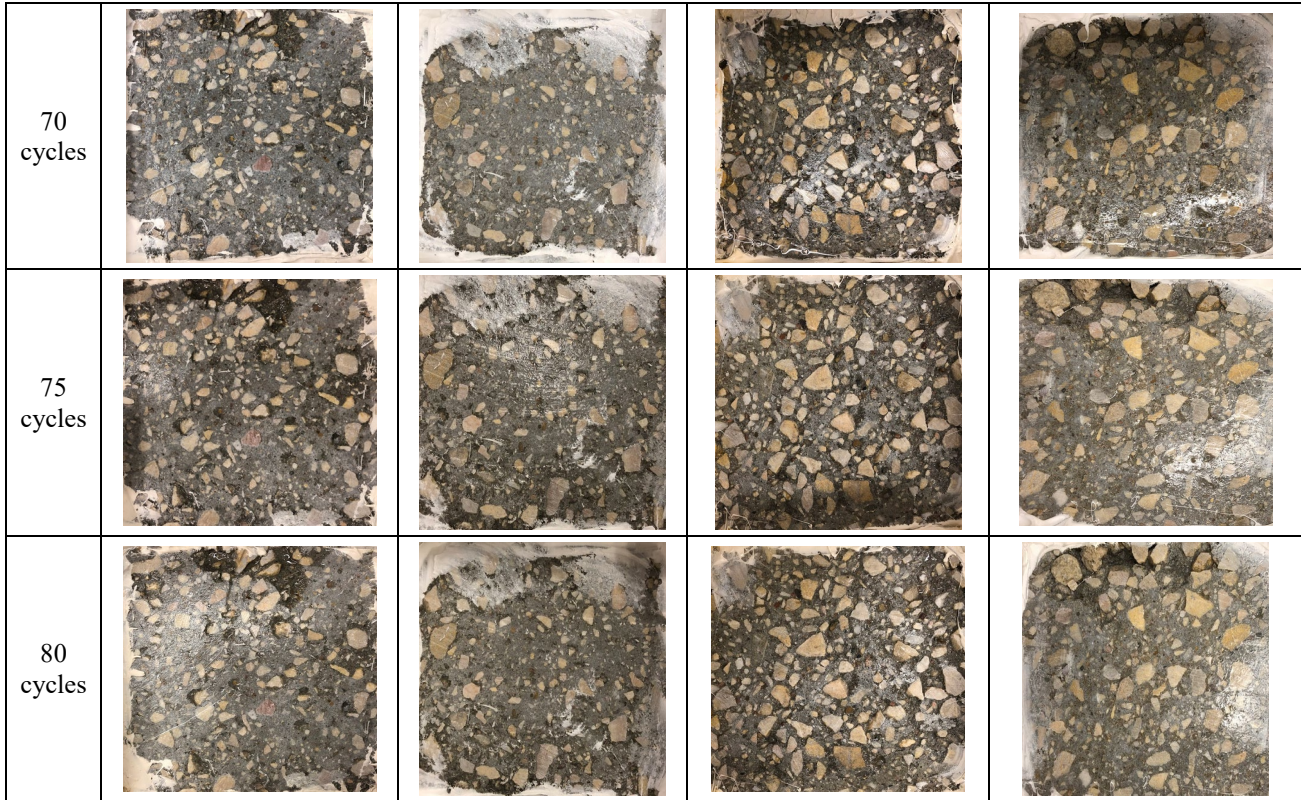


Figure 30 shows the cumulative mass loss of the two mixtures during salt scaling test after 80 freeze-thaw cycles.

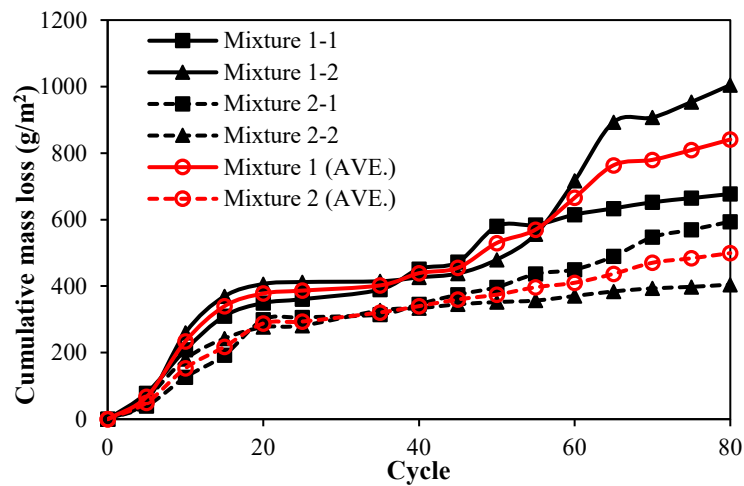


Figure 30 – Weight loss of saw-cut slabs after different cycles

The cumulative mass loss increased rapidly with the increase of freeze-thaw cycles. The scaled-off mass collected from the Mixture 1 was noticeably higher than that of the Mixture 2, especially after 35 cycles, which was around 0.17 lb/ft² (840 g/m²) compared to 0.10 lb/ft² (500 g/m²) in the case of the mixture with fibers. However, the weight loss recorded for both mixture (with and without fibers) were below the acceptable range of 0.20 lb/ft² (1000 g/m²) at 50 cycles, which is mainly attributed to the high surface density of mixtures due to the compaction during paving.

4.9. Drying shrinkage

Drying shrinkage of mixtures was determined for saw-cut prisms measuring 3"× 3"×11.3" according to ASTM C157 using a digital type extensometer (DEMEC gauge). Shrinkage of saw-cut prisms was measured during 180 d in a temperature of 70 ± 3 °F and relative humidity of $50\% \pm 4\%$. Figure 31 shows the shrinkage setup used and mass loss measurement of investigated samples.

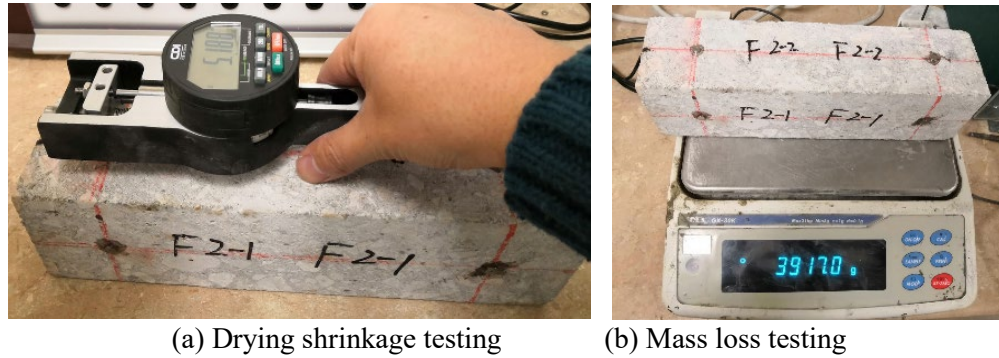


Figure 31 - Drying shrinkage and mass loss measurement

Figure 32 shows the variation of drying shrinkage of the two investigated mixtures up to drying time of 180 days.

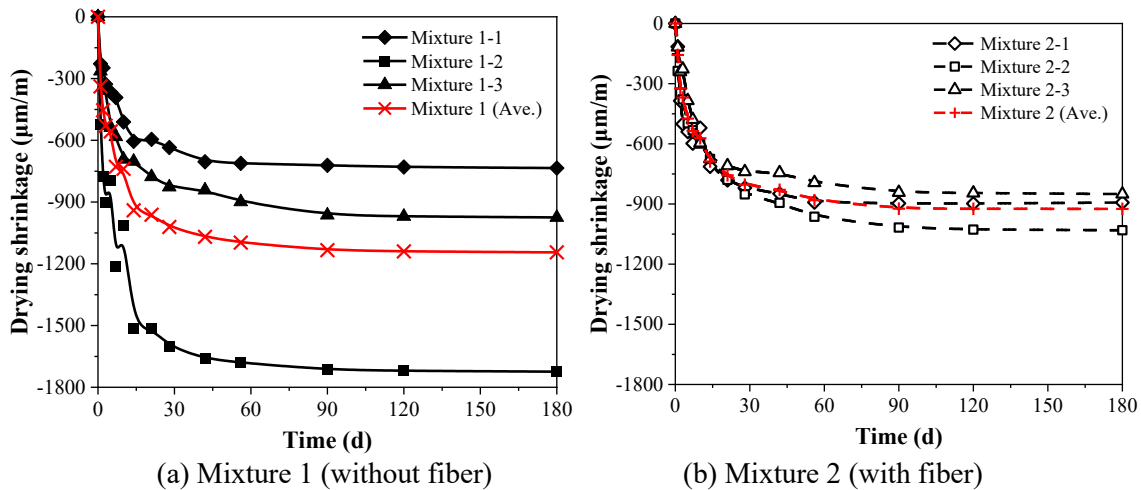


Figure 32 - Variations of drying shrinkage determined on saw-cut samples

The concrete made without fibers had very large spread of shrinkage performance, as indicated in Figure 32 (a). This may be due to large variation in consolidation among the three saw cut samples or due to movement in the DEMEC point that was glued to the sample shortly before the beginning of testing. By ignoring the lowest shrinkage sample, the average the two remaining samples would be similar to those of the fiber-reinforced CCP. The incorporation of 5 pcy of synthetic fibers restricted shrinkage, and all three samples had similar performance. The non-fibrous mixture had drying shrinkage of 1125 micro-strain when all three test samples were considered, compared to 900 micro-strain in the case of mixture with fibers.

5. Cell performance

5.1. Curling and warping

The curling and warping measurements were conducted as per ASTM E1364 on December 19th, 2018 and September 27th, 2019. For all three CCP cells (Cells 1, 2, and 3). curling and warping measurements were conducted in the longitudinal, transverse, and diagonal directions (Figure 32). Both morning and afternoon measurements were taken on the day of testing to obtain values under variable temperature and moisture conditions.

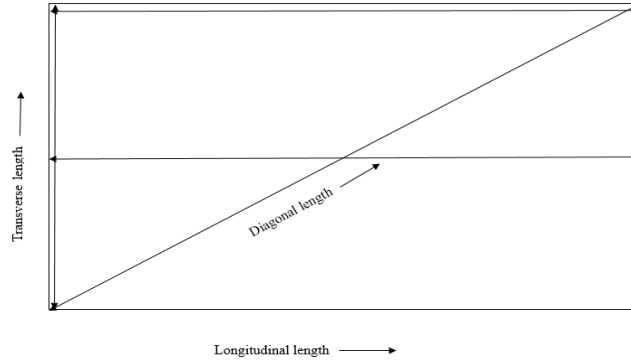


Figure 33 - Direction of measurements - longitudinal, diagonal, and transverse lengths.

Figure 34 shows the testing equipment for curling and warping measurements, which comprised of two steel columns (A and B) connected with metal string adjusted and tightened with roller components of the columns.



Figure 34 - Test setup and measuring equipment

The test was developed by Iowa State University. For precise measurement, columns A and B were anchored at joints (discontinuities between two cells), as shown in Figure 32. Then the string was hooked off from column A and drawn to pass through the roller in column B. After that, the string was tightened firmly by adjusting a handle in column B. Two pins were placed under the string to make it stretched to avoid formation of sagging of string. A measuring tape was spread out along the string to record the locations of measured points. Prior to curling and warping

measurements, the pavement surface was cleaned, and temperature and ambient relative humidity (RH) were recorded and tabulated, as reported in Table 13.

Table 13 - Temperature and relative humidity data

| Date | Time | Temperature (°F) | Relative humidity (%) |
|------------|-----------|------------------|-----------------------|
| 12/19/2018 | Morning | 49 | 66 |
| | Afternoon | 53 | 69 |
| 09/27/2019 | Morning | 84 | 60 |
| | Afternoon | 88 | 53 |

The measurement was conducted at a maximum measuring interval of 2 ft (610 mm) for Class 2 resolution (ASTM E1364). However, at critical locations of curling and warping (e.g., cell edges and center) intervals of 2 in. measurements along the profile were taken. A digital height gauge was used as a measuring gauge considering its convenient operation in the field. The data were collected at eye level to the string.

Figures 35 – 38 compare curling and warping readings of Cells 1 and 3 (with and without fibers) and Cells 1 and 2 (without fibers with different panel sizes) measured on 12/19/18 and 09/27/19 in four reading directions. The results showed that the cell with fibers (Cell 3) had more significant deflection at early age, especially those recorded in the diagonal direction. As can be seen from Figure 5, the deflection readings of Cell 3 ranged from -1.25 to 0.5 in. These readings were limited to -0.5 to 0.5 in. for Cells 1 and 2. The increased deflection of Cell 3 can be related to higher crack resistance developed by fiber reinforcement. Possible formation of microcracks in Cells 1 and 2 (without fibers) can increase the degree of freedom of the system and reduce the deformation. On the contrary, comparing results from Cells 1 and 2 (Figure 38) shows that the size of the cells had negligible influence on curling and warping deflection.

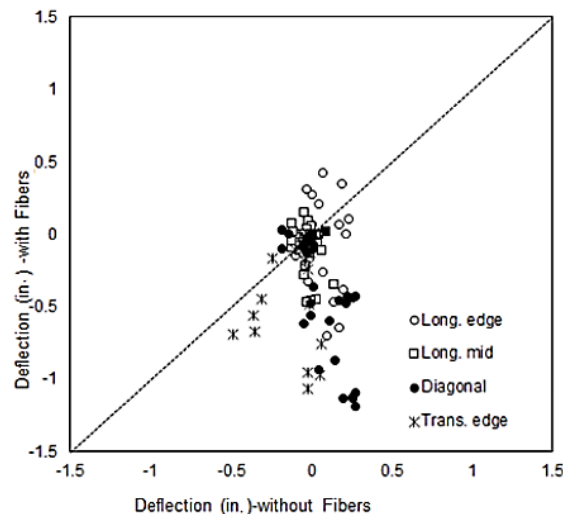


Figure 35 - Deflection (in.) of cells cast with fibers vs. those without fibers measured on 12/19/18

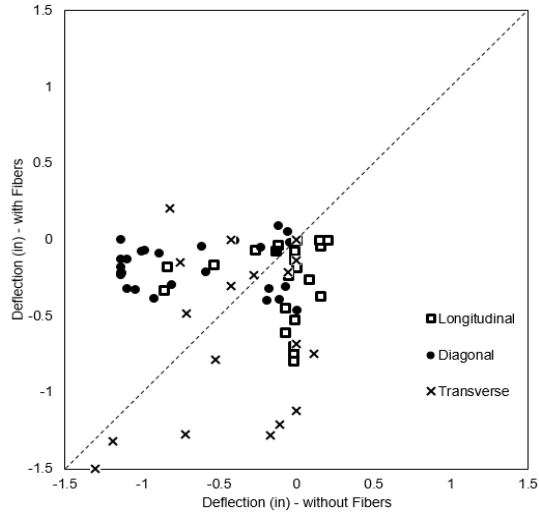


Figure 36 - Deflection (in.) of cells cast with fibers vs. those without fibers measured on 09/27/19

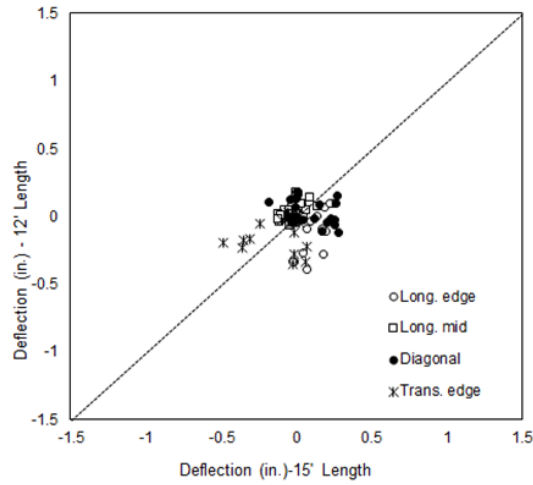


Figure 37 - Deflection (in.) of cells cast without fibers with L=12' (Cell 1) vs. L=15' (Cell 2) measured on 12/19/18

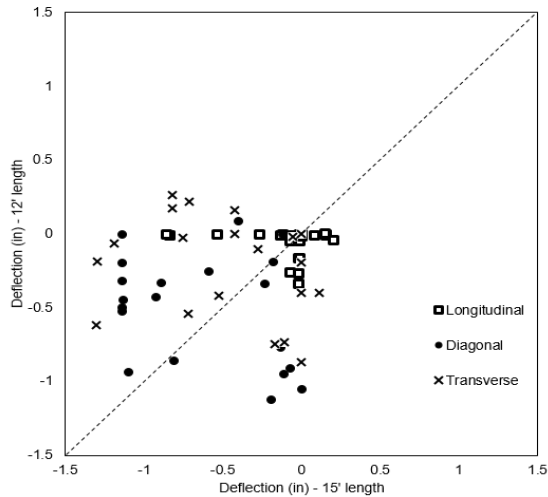


Figure 38 - Deflection (in.) of cells cast without fibers with L=12' (Cell 1) vs. L=15' (Cell 2) measured on 09/27/19

5.2. Environmental performance (analysis of MnDOT data)- Oct. 2018- Dec. 2019

The analysis of MnDOT environmental and load response performance data includes the readings of three typical sets of sensors located at three different stations (551, 552, and 553) in three CCP cells. The data includes the readings of three typical set of sensors located at three different stations, 551, 552, and 553, in a compacted concrete pavement (CCP) slab section. In this project, the sensors include two vibrating wire gauges aligned in the longitudinal and the transverse directions, as well as two thermocouples located at the top and the bottom of the CCP slab section (See Figure 9).

The adjusted temperature readings of the thermistors (XV) attached to the top and the bottom of the slab section at the three investigated stations 551, 552, and 553 are plotted separately in Figures 39, 40, and 41 and combined in Figure 42. The thermocouples readings at the top section of the three stations were referred to as XV 551-1, XV 552-1, and XV 553-1, while the bottom readings of the three stations were referred to as XV 551-2, XV 552-2, and XV 553-2.

During the winter, the temperature varied between -2 and 22 °C (72 and 28 °F), where the temperature reached its maximum value after approximately 24 hours of concrete placement. During the summer, the temperature varied between 25 and 45 °C (77 and 113 °F), where the temperature reached its maximum value at the first week of August. The temperature variation between the top and the bottom of the slab was not significant, where a maximum temperature variation of 5 °C (41 °F) was recorded in August at station 551.

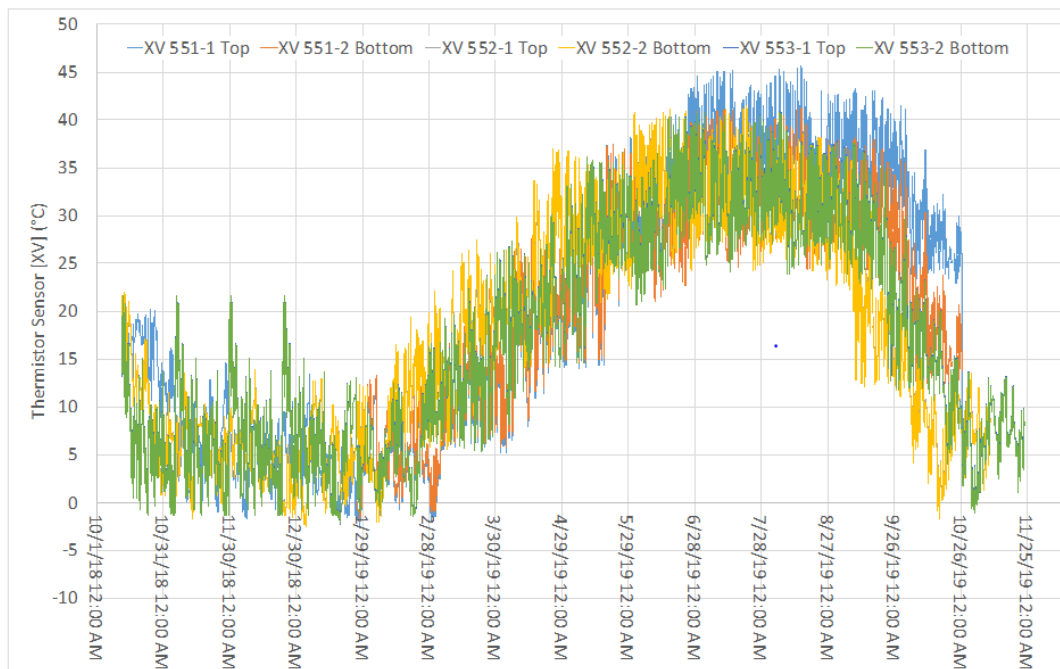


Figure 39: Temperature readings of the thermistors attached to the top and the bottom of the slab section at station 551.

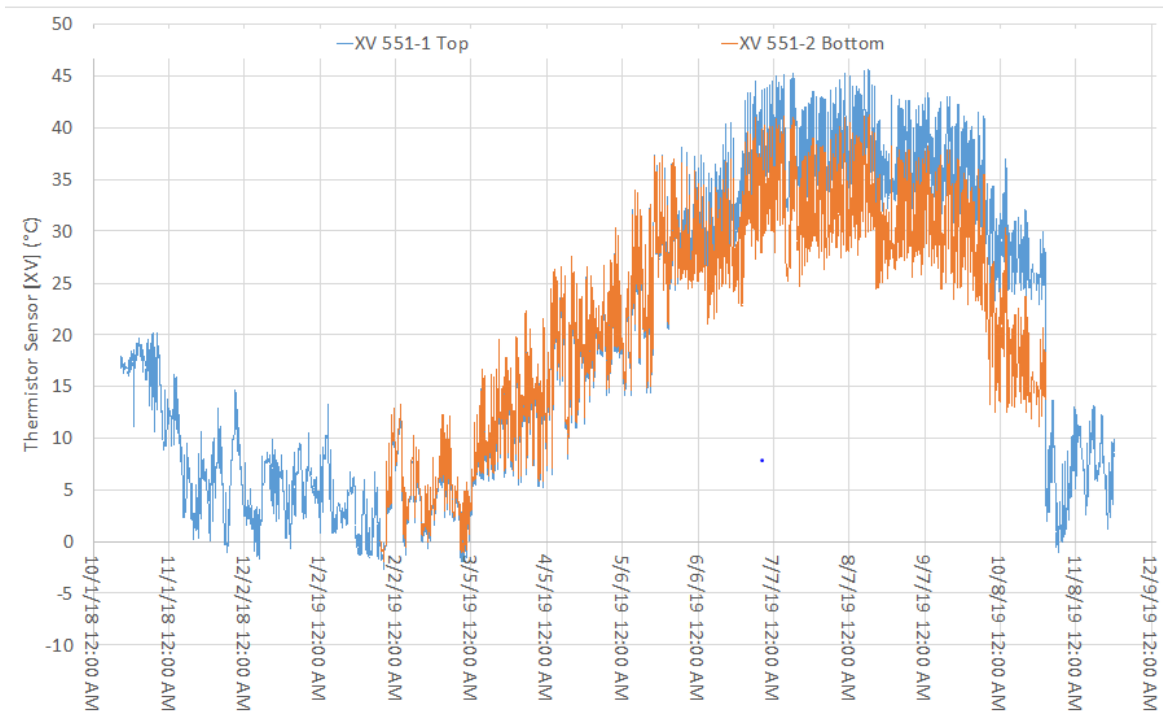


Figure 40: Temperature readings of the thermistors attached to the top and the bottom of the slab section at station 552.

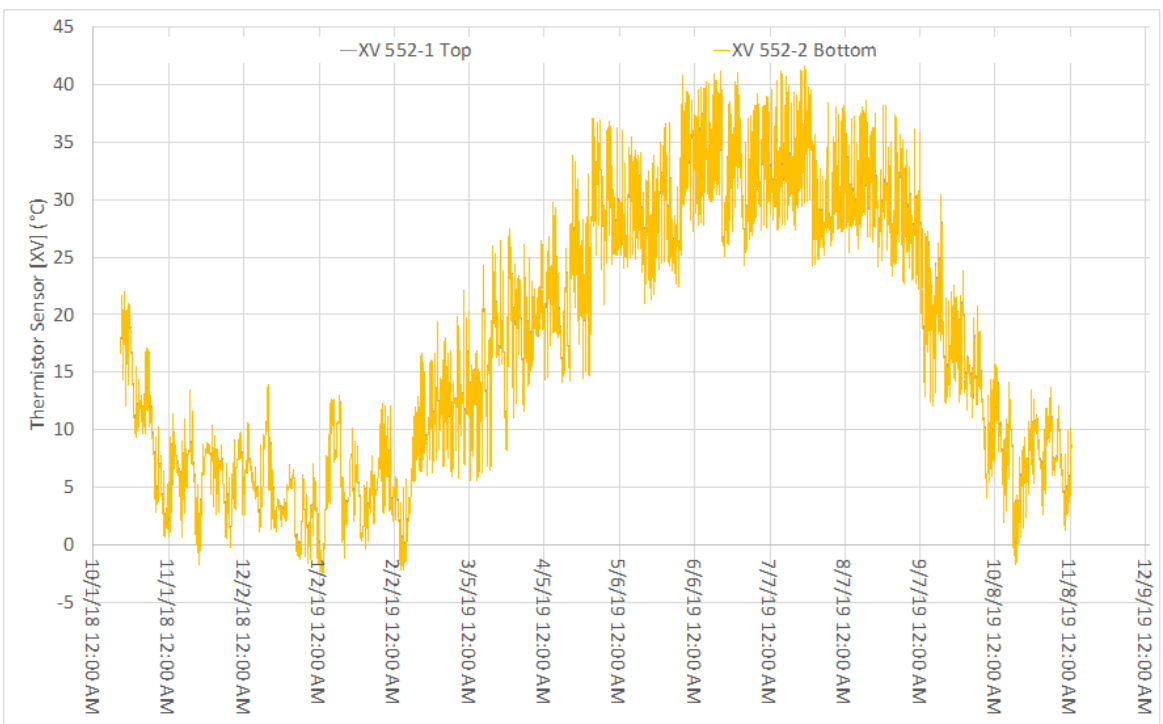


Figure 41: Temperature readings of the thermistors attached to the top and the bottom of the slab section at station 553.

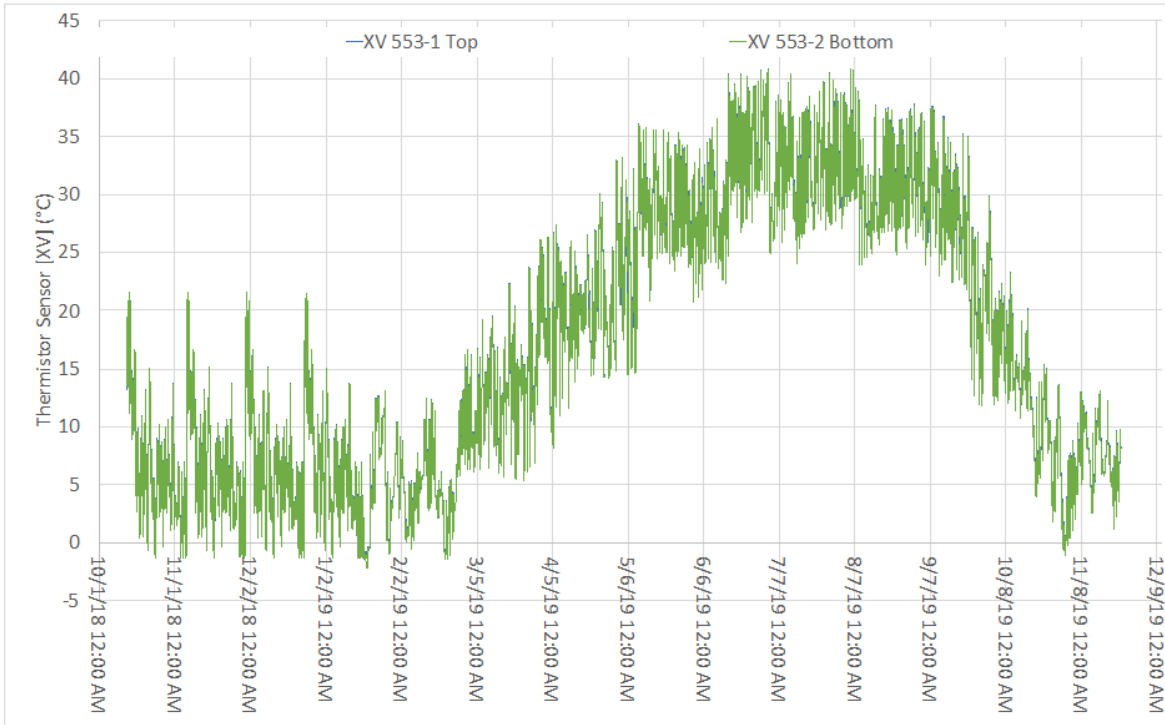


Figure 42: Temperature readings of the thermistors attached to the top and the bottom of the slab section at the three investigated stations.

The temperature variations between the top and the bottom sections at the three investigated stations are plotted in Figure 43. The temperature variation at the three investigated stations was found to reach zero on 10/12/2018 between 2:00 pm and 3:00 pm, which indicated that the concrete had hardened sufficiently to fully engage the sensors and the initial vibrating wire strain gauge (VW) values were considered.

Figure 44 shows the strain variations of the longitudinal and the transverse directions of the investigated three stations that were referred to as VW 551-1, VW 551-2, VW 552-1, VW 552-2, VW 553-1, and VW 553-2, respectively. After approximately seven weeks of concrete placement, the longitudinal and the transverse sections reached a maximum strain of 960 and 940 micro-strains, respectively. Generally, the strain varied between 850 and 960 micro-strains. Both longitudinal and transverse strains went down in summer, reaching lowest values first week of July. The strains after that started to go up. The rate of decrease of the transverse strain was much lower than the longitudinal strain. For example, at Station 551 the longitudinal strain was higher than the transverse strain up first week of May then the transverse strain started to be higher than the longitudinal one.

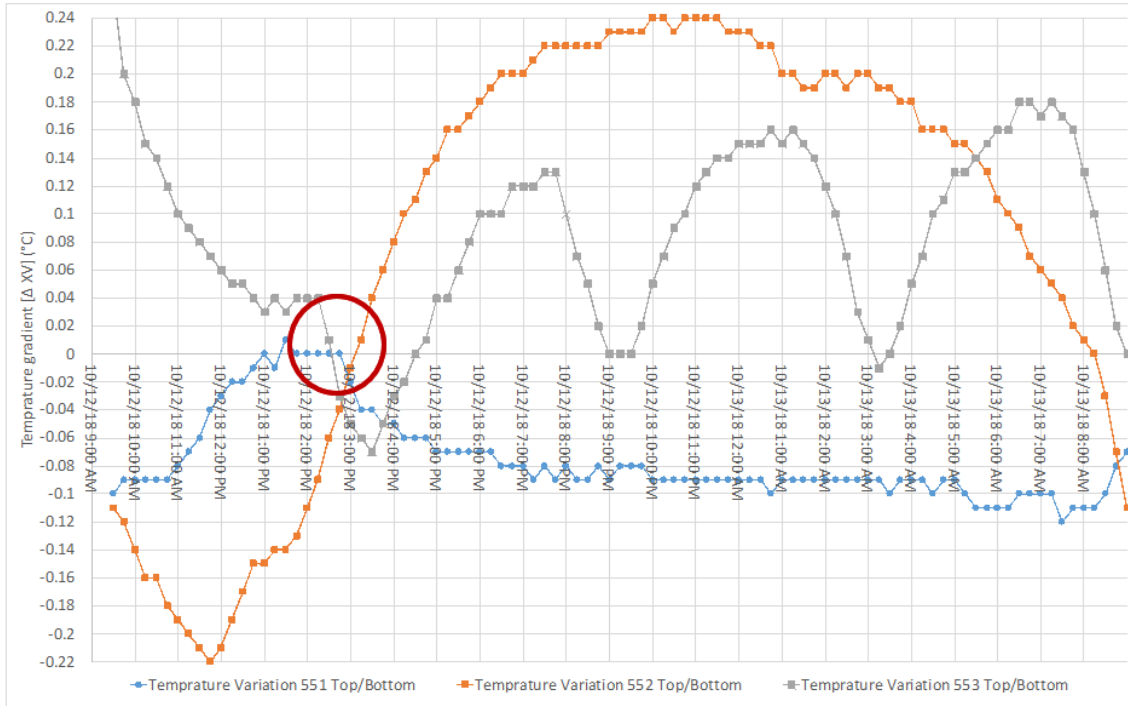


Figure 43: Temperature variations between the top and the bottom sections of the three investigated stations.

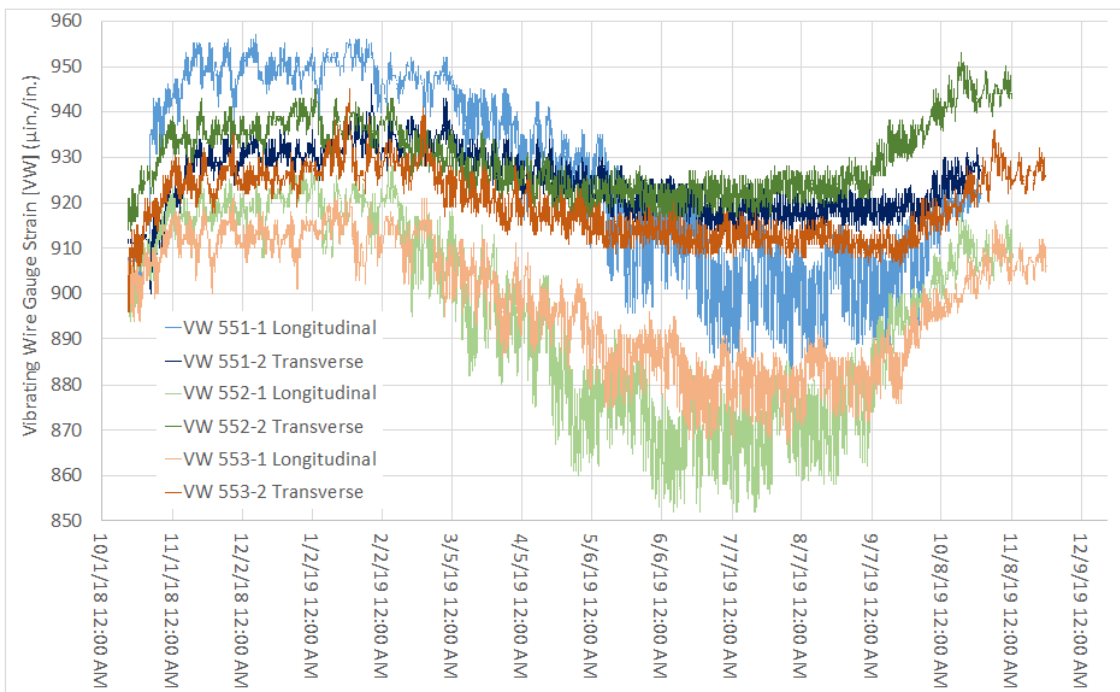


Figure 44: Strain variations at the longitudinal and the transverse directions of the three investigated stations.

6. Concluding remarks

In this study, the performance of designed CCP mixtures with and without fibers were determined. The primary performance characteristics included mechanical properties, drying shrinkage, durability, and enhancement of joint load transfer gained from fiber-reinforcement of the pavement. The results showed that incorporation of 5% pcy fibers did not show significant improvement on flexural performance and frost durability, however, the restraining effect of fibers on the drying shrinkage was noticeable. The main concluding remarks of the study is listed below:

1. Based on the Vebe consistency time results for representative samples, both tested mixtures (with and without fibers) are categorized to have extremely dry consistency. The test results showed that the incorporation of fibers increased the density of the fresh CCP by 15%.
2. The compressive strength of mixture with 5% pcy fiber was greater than that of samples without fiber. Results showed that the compressive strength of cast-in-field samples was higher than that of saw-cut samples. For example, the compressive strength of 91d cast-in-field Mixtures 1 and 2 was 41% and 39% greater than that of saw-cut specimens, which indicates that the rate of compaction was higher in cast-in-field samples that that applied by the paver.
3. The incorporation of 5% pcy fibers slightly increased flexural strength for cast-in-field samples but reduced that for saw-cut samples. For example, the incorporation of fiber increased the flexural strength from 555 to 685 MPa for cast-in-place samples, while using fiber in saw-cut specimens decreased flexural strength from 404 to 295 MPa. However, the prolonged curing time increased the flexural strength. The incorporation of 5% pcy fibers improved post-cracking behavior.
4. The incorporation of 5% pcy fibers in saw-cut samples led to 35% increase in the chloride permeability.
5. The use of 5% pcy fibers slightly resulted in 5% and 15% decrease in the bulk and surface electricity resistivity, respectively.
6. Mixtures made with 5% pcy fiber had an air content of 5.12% compared to 4.03% for plain mixture. The spacing factor also increased from 0.006 to 0.007 due to the use of 5% pcy fiber.
7. Mixtures prepared with and without pcy fiber had a similar freezing-and-thawing durability.
8. No visible scaling was observed during 80 cycles indicating acceptable resistance of the two mixtures to salt scaling. After 80 freeze-thaw cycles, the cumulative mass loss increased rapidly with the increase of freeze-thaw cycles, and the obvious surface degradation can be observed.
9. The incorporation of 5% pcy fibers restricted shrinkage. The non-fibrous mixture had drying shrinkage of 1125 micro-strain, compared to 900 micro-strain in the case of mixture with fibers.
10. The curling and warping in the pavement sections increased over time. No significant difference in deflection were observed between fiber-reinforced and non-fiber reinforced cells.

7. Additional Notes:

1. This project is still underway with the other sponsor, Missouri Department of Transportation, and the final results will be published at the end of that period. The final report will be uploaded on the RE-CAST project website at:
<https://recast.mst.edu/projects/compactedconcretepavement/>
2. The remaining portion of the work is scheduled to be completed by 12/31/2021.